Numerical and theoretical calculation of breakdown voltage in the electrical discharge for rare gases

Fatiha Ghaleb [a] & A. Belasri [a]

[a] Laboratory of Plasma Physics, Conducting Materials and their Applications Faculty of Science, Department of Physics , USTOMB , Oran , Algeria
Published online: 24 Feb 2012.

PLEASE SCROLL DOWN FOR ARTICLE

Taylor & Francis
Taylor & Francis Group

Numerical and theoretical calculation of breakdown voltage in the electrical discharge for rare gases

Fatiha Ghaleb* and A. Belasri

Laboratory of Plasma Physics, Conducting Materials and their Applications Faculty of Science, Department of Physics, USTOMB, Oran, Algeria

This work has been devoted to a numerical and analytical calculus of the voltage breakdown in electrical discharge for several rare gases such as argon, krypton, neon, xenon and helium. It was performed using a fluid model 2D, which is based on the numerical solution of the two Boltzmann equations (equation of continuity and momentum), coupled to Poisson's equation to measure the breakdown voltage according to the product of the electrode spacing and the pressure. This study allowed a better comprehension of the physical phenomena occurring in the discharges. We, thus, developed a calculation, based on the empirically Paschen's law, allowing the determination of the breakdown voltage, which describes the transition from insulating gas to the conductive state. Paschen's curves of the different gases are plotted and a comparison between numerical and experimental as well as analytical results is also presented and analyzed.

Keywords: electrical discharge; fluid model; analytic model; Paschen's curves; breakdown voltage

1. Introduction

Gas breakdown is the process that occurs when an electrically neutral gas absorbs enough energy for it to become ionized and electrically conducting. In laboratory plasmas, this is usually achieved by placing a large voltage across two electrodes: the applied electric field accelerates stray charges and begins the breakdown process (*1*). Plasma breakdown, also referred to as plasma ignition, is an important fundamental process in plasma science and has a long history of study. It started in the late nineteenth century, Paschen (*2*) was the first scientist to study the electric breakdown of dielectric gases between metallic electrodes, and then formulated the so-called Paschen's law which has been so effective in the prediction of electrical breakdown of gases. Recently, the breakdown physic has known more interest (*3–5*), because many plasma applications are influenced by this process, and its understanding is very necessary for the development of these devices and particularly for the optimization of the energy used. Such applications are diverse, including cleaning of exhaust gases (*6*), ignition of light sources (*7, 8*) and material processing using pulsed plasma sources (*9, 10*). Although the breakdown theories are appropriate for many developed situations (*11*) known, some physics and kinetics aspects are poorly understood. For the

*Corresponding author. Email: ghaleb.fatiha@gmail.com

more complicated discharge systems used in many applications, it is very difficult to predict the general features such as the timing of the breakdown and the necessary voltage. For this reasons, several numerical and theoretical (12–14) works are developed to understand the breakdown mechanism. The main aim of this work is to calculate the breakdown voltage in electrical discharge, using a rare gas and to understand how the discharge geometry and other parameters affect these processes. The simulation code used in this work is the matrix AC-PDP (two-dimensional) (15); the breakdown voltage as a function of the p.d (pressure times electrode distance) product are calculated. This Paschen's curve represents a balance between the number of electrons lost by diffusion and drift in the inter-electrode gap and the number of secondary electrons generated at the cathode (16).

The 2D fluid and analytic model used in this study are described in Sections 2 and 3, respectively. In Section 4 are discussed the results obtained from the two models. Concluding remarks are presented in Section 5.

2. 2D fluid model

In this work, a fluid model in two dimensions was used (15). The model is based on solving the first two moments of the Boltzmann equation and the Poisson equation using the finite difference scheme (17, 18). The two Boltzmann equations (equation of continuity and momentum) and Poisson's equation are represented by

$$\frac{\partial n_{e,p}}{\partial t} + \vec{\nabla}.n_{e,p}v_{e,p} = S_{e,p}, \tag{1}$$

$$n_{e,p}\bar{v}_{e,p} = an_{e,p}\mu_{e,p}E - \vec{\nabla}.(D_{e,p}n_{e,p}), \tag{2}$$

$$\vec{\nabla}.\varepsilon_r E = \frac{e}{\varepsilon_0}(n_p - n_e), \tag{3}$$

where n is the density of charged particles (e for electrons, p for positive ions or negative). S is the source term of the equation of continuity, he reports the creation (ionization) and losses (attachments, recombination) of charged particles, $\bar{v}_{e,p}$ represents the average speed, E the electric field, $\mu_{e,p}$ is always positive corresponding to the mobility of electrons and ions, $D_{e,p}$ is the diffusion coefficient, and ε_r and ε_0 are the dielectric and vacuum permittivity, respectively.

The breakdown is said to occur when the maximum total ion density reaches a given value within a given time interval. The result will obviously depend on the initial electron and ion density (supposed to be uniform in the gap). The initial density is equal to $10^4\,\mathrm{cm}^{-3}$ and the maximum total ion density at breakdown is $10^{11}\,\mathrm{cm}^{-3}$. The design of the 2D discharge cell is shown in Figure 1. The dielectric covering of the electrodes has a relative permittivity of 10. These electrodes are separated by a distance of 0.05 cm. This space is filled by various different rare gases.

3. Analytical model

The analytical model (19) based on the Paschen's laws is developed for the obtaining of the breakdown voltage curve, which represents a balance between the number of electrons lost by diffusion and drift in the inter-electrode gap and the number of secondary electrons generated at the cathode (20). Over a large range of pressures and electrodes separation, the probability of ionization per electron–neutral collision in the gas and the probability of the production of
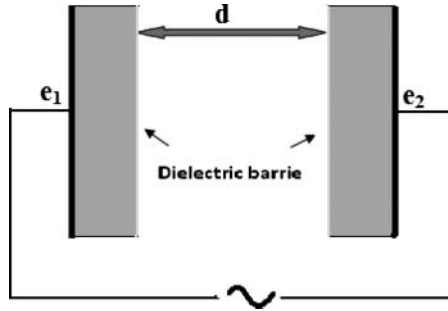
Figure 1. The geometry of the discharge cell.

secondary electrons by ion bombardment of the cathode are proportional to the reduced field (*21*) and lead to the well-established *pd* similarity law.

Indeed, the Paschen's law, which represents the breakdown voltage of a gas in the homogeneous field, induces the verification of the self-sustained condition (Equation (4)). It should be noted that the existence of breakdown voltage depends on a critical number of electron multiplications throughout the ionization process induced by collisions between electrons and gas molecules in the inter-electrode distance (*22, 23*).

$$M = \exp(\alpha d) = 1 + \frac{1}{\gamma}, \tag{4}$$

where M is the multiplication factor, γ is the secondary electron emission at the cathode and α is the first Townsend coefficient indicated by the Equation (5) (*24, 25*).

$$\frac{\alpha}{p} = D_1 \exp\left[-D_2 \left(\frac{p}{E}\right)^{0.5}\right], \tag{5}$$

where α is the number of ionizing collisions per unit length, E the electric field, (D_1 and D_2) are positive constants, dependent on the gas composition. It can be deduced by experimental measurements (*26*) or by numerical and analytical calculations (*27–30*).

The expression of the electric field is

$$E_b = \frac{V_b}{d}. \tag{6}$$

In plane geometry, the breakdown voltage V_b is given by Equation (7) (*31–33*).

$$V_b = \left|-\left[\frac{pdD_2^2}{(\ln(M/D_1pd))^2}\right]\right|. \tag{7}$$

This equation represents the general formula of the breakdown voltage of pure gases. It seems that the breakdown voltage will be proportional to *p.d*. This is equivalent to the breakdown condition being a constant value of E_b/p for a given gas, and is consistent with E/p being a measure of the average energy gain of an electron between collisions. For this case, electrons make many collisions, and therefore the breakdown condition is equivalent to a constant value of the energy gained by an electron between collisions. This means that the electric field must scale linearly with the pressure, or V_b is linear in *p.d*. At very small values of *p.d*, there are very few collisions, and therefore, V_b the breakdown voltage rises to increase the probability of breakdown per collision. The minimum breakdown voltage is called the Paschen's minimum.

4. Results and discussion

Our stated goal in this paper is to compare the different Paschen's curves obtained for xenon, neon, argon krypton and helium by resolving the fluid model and the analytical model described in the previous section. In Figure 2, we have shown the calculated results of the breakdown voltage in xenon compared to those obtained by experiment resuls (*34*, *35*). It seems that the breakdown voltage increases linearly with the *p.d* product and the xenon plasma exhibits a maximum breakdown voltage when this product is equal to 10 Torr cm. We observe a good agreement between the numerical and the experiment results as well as with the analytical model results when the multiplication factor *M* is equal to 10^3 and 10^4.

The results displayed in Figure 3 have been obtained in neon. We see from this figure that the minimum value of the breakdown voltage is in the order of 150 V when the product *p.d* is equal
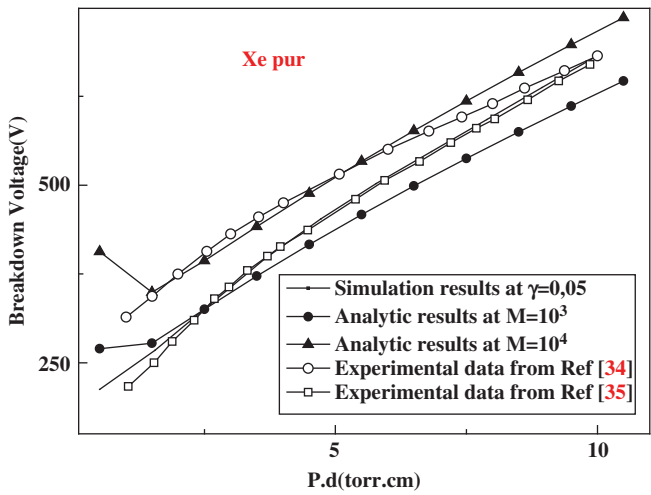

Figure 2.   Breakdown voltage in xenon as a function of the product (*p.d*). Line presents fluid calculation 2D, theoretical results are given by solid symbols, while the results of measurements taken from (*34*, *35*) are shown by open symbols.
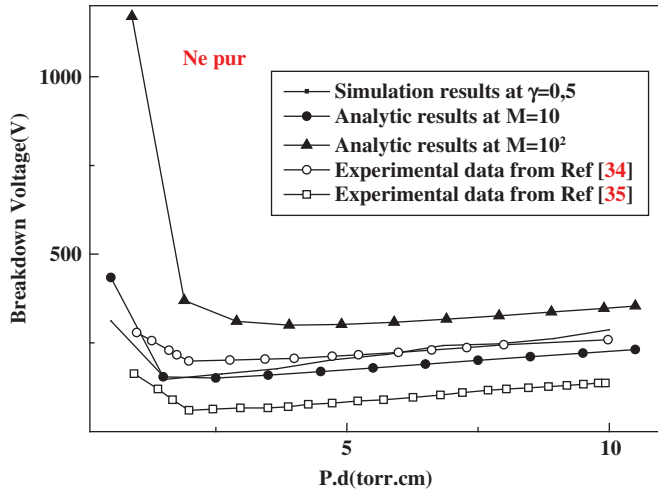

Figure 3.   Dependence of the breakdown voltage on the pressure–gap spacing product in neon. Solid symbols correspond to the analytic result which are obtained by the resolution of the self-sustained equation, the simulation results are obtained by line and open symbols corresponding to the results of experimental measurements (*34*, *35*).

to 2 Torr cm. Nevertheless, it should be pointed out that the Paschen's curves obtained have the same behavior with adjustments of increase and reduction in the breakdown voltage.

Figure 4 shows the simulation results obtained in argon by using the 2D code and the analytical model (solid symbols) are compared with the experimental data (open symbols) taken from (*34*, *35*). In Figure 5 the plots of simulation and analytical results are illustrated and compared to those reported in (*34*, *35*) for krypton. The simulation results were obtained, including the emission effect and show relatively good agreement with the available experimental results. Differences that can be observed between simulation and experimental results could be explained by the fact
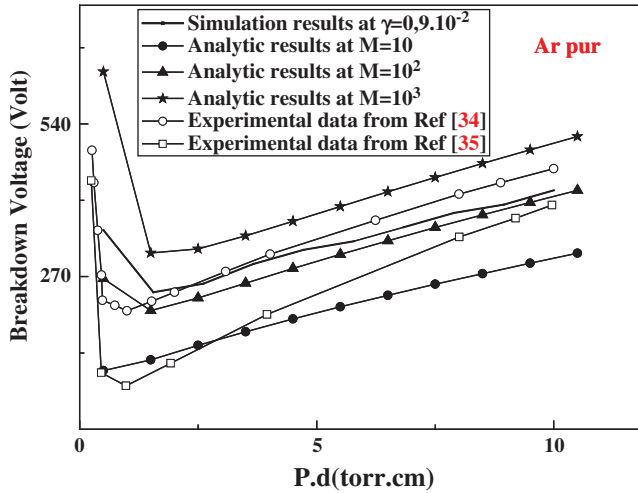

Figure 4. Comparison of the breakdown voltage according to the product *p.d*, between the analytical model and the fluid model for argon, the curves with solid symbol were calculated by solving condition of self-sustaining for different electronic multiplication, they are analytical calculations, and the curve without symbols corresponds to the numerical results which are calculated by the model 2D, and the two other curves represented by open symbols (circle and square) are calculated by measurements of the experiment (*34*, *35*), respectively.
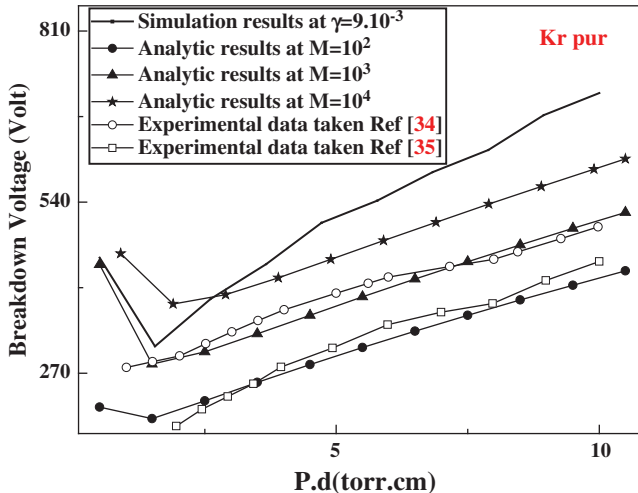

Figure 5. Breakdown voltage measurements as a function of pressure and gap spacing in pure krypton. The solid symbols represent the analytical calculation, and the numerical results indicated by line, or the secondary electron emission coefficient for krypton ions is set to 0.1, whereas the open symbol indicates experimental results (*34*, *35*).
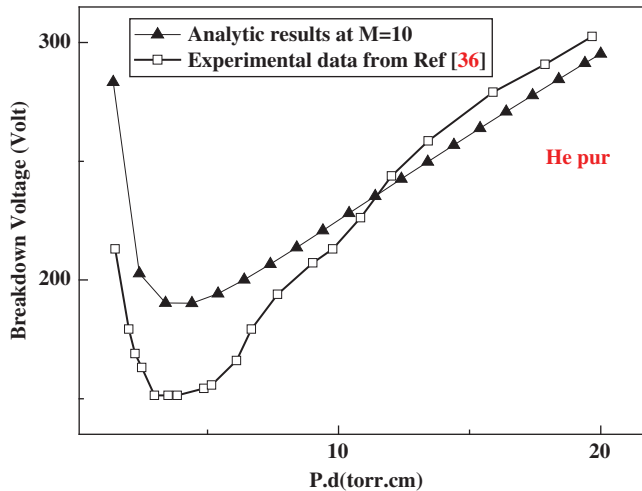
Figure 6. Plots of measured breakdown voltages versus product of the pressure and the width gap between electrodes in helium. The triangular symbols are the analytical data measured by resolving the equation of self-sustaining for electronic multiplication equal to 10; the square symbols are experimental data obtained (*36*).

that except slightly different operating conditions between the experiment and the simulation. Since the breakdown voltage strongly depends on the electrode material and surface conditions, the onset of them can cause disagreement between simulation and experimental results. The model results overlap with the results of the theory for weak products *p.d*, and for high products the breakdown voltage in simulation becomes very large because of electron losses by diffusion and absorption by the cathode. Curves of the breakdown voltage obtained from the Paschen's law for pure helium are shown in Figure 6. The triangle symbol shows analytical results obtained at the $M = 10$, while the square symbol corresponds to the results of experimental calculations (*36*). One can see that the breakdown voltage cure predicted with the analytical model has the same wave form as that found in the experimental work, and when the critical value of the electric field is achieved, the increase of the breakdown voltage with the pressure is slower than that predicted by Paschen's law.

5. Conclusion

The aim of the present work is the calculus of the breakdown voltage curves for neon, xenon, krypton, argon and helium. For this purpose, two different models were used: the analytical model is based on the self-sustaining equation, and a 2D fluid model based on the two first moment equations for electrons and ions transport coupled with Poisson's equation, in the case of plan–plan geometry. The predicted breakdown voltage curves have the same wave forms as that obtained from several experimental works. However, recent technologies use complex geometries and different gas mixtures need the introduction of other parameters in breakdown voltage calculation and thereby to the improvement of the Paschen's law.

Acknowledgements

References

(1) Jiang, T. Stark Spectroscopy on Rare Gas Atoms. Ph.D. Thesis, Eindhoven University, Eindhoven, 2006.
(2) Paschen, F. *Wied. Ann.* **1889,** *37,* 69–96.
(3) Xiong, J.; Zhou, Z.; Ye, X.; Wang, X.; Feng, Y. *Sens. Actuators, A* **2003,** *108,* 134–137.
(4) Madou, M.J. *Fundamentals of Microfabrication: The Science of Miniaturization*; CRC Press: Boca Raton, FL, 2002; p. 551.
(5) Ching-Heng, C; Andrew, Y.J.; Wang, P.-J. *J. Micromech. Microeng.* **2006,** *16,* 1366–1373.
(6) Van Veldhuizen, E.M. *Electrical Discharges for Environmental Purposes: Fundamentals and Applications*; Nova Science Publishers: Huntington, NY, 2000.
(7) Horstman, R.E.; Oude Lansink, F.M. *J. Phys. D: Appl. Phys.* **1988,** *21,* 1130–1136.
(8) Brok, W.J.M.; van Dijk, J.; Bowden, M.D. et al. *J. Phys. D: Appl. Phys.* **2003,** *36,* 1967–1979.
(9) Sugai, T.; Yoshida, H.; Shimada, T. et al. *New Nano Lett.* **2005,** *3,* 769–773.
(10) Dorai, R.; Kushner, M.J. *J. Phys. D: Appl. Phys.* **2002,** *35,* 2954–2968.
(11) Momćilo Pejović, M.; Goran Ristić, S.; Jugoslav Karamarković, P. *J. Phys. D: Appl. Phys.* **2002,** *35,* R91–R103.
(12) Punset, C.; Cany, S.; Boeuf, J.P. *J. Appl. Phys.* **1999,** *86,* 124–133.
(13) Ikeda, Y.; Suzuki, K.; Fukumoto, H. et al. *J. Appl. Phys.* **2000,** *88,* 6216–6223.
(14) Yang, S.; Kim, H.C. et al. *IEEE. Trans. Plasma. Sci.* **2003,** *31,* 596–605.
(15) Belasri, A.; Benstâali, W.; Haffaf, H. *Rev. Energ. Ren.* **2003,** *6,* 35–43.
(16) Radmilović-Radjenović, M.; Radjenović, B. *Contrib. Plasma Phys.* **2007,** *47,* 165–172.
(17) Ganter, R.; Callegari, T.; Pitchford, L.C.; Boeuf, J.P. *Appl. Surf. Sci.* **2002,** *192,* 299–308.
(18) Punset, C.; Boeuf, J.P.; Pitchford, L.C. *J. Appl. Phys.* **1998,** *83,* 1884–1897.
(19) Ghaleb, F.; Benstâali, W.; Belasri, A. *J. Mater. Sci. Eng. C* **2008,** *28,* 791–794.
(20) Meek, J.M.; Craggs, J.D. *Electrical Breakdown of Gases*; Oxford University Press: Oxford, 1953.
(21) Loeb, L.B. *Fundamental Processes of Electrical Discharges in Gases*; Wiley: New York, 1939.
(22) Uhm, H.S. et al. *J. Phys. Plasmas* **2005,** *12,* 033507-1–033507-9.
(23) Nasser, E. *Fundamentals of Gaseous Ionization and Plasma Electronics*; Wiley-Interscience: New York, 1971; p. 219.
(24) Mankowski, J.J. High Voltage Subnanosecond Dielectric Breakdown. Ph.D. Thesis, Texas Tech University, Lubbock, TX, 1997.
(25) Diver Declan, A. *A Plasma Formulary for Physics, Technology and Astrophysics*; Wiley-VCH Verlag GmbH: Berlin, 2001.
(26) Huxley, L.G.H.; Crompton, R.W. *The Diffusion and Drift of Electron in Gases*; Wiley: New York, 1974.
(27) Pitchford, L.C.; Oneil, S.V. et al. *Phys. Rev. A* **1981,** *23,* 294–304.
(28) Ségur, P. et al. *Transp. Theory Stat. Phys.* **1986,** *15,* 705–757.
(29) Naidu, M.S.; Kamaraju, V. *High-Voltage Engineering*; McGraw-Hill Companies: New York, 2009.
(30) Raizer, Yu.P. *Gas Discharge Physics*; Springer: Berlin, 1991.
(31) Ray, S. *An Introduction to High Voltage Engineering*; Prentice Hall of India: New Delhi, 2004.
(32) Radmilović, M.; Radjenović, B.; Petrović, Z. et al. *Czech. J. Phys.* **2006,** *56,* B996–1001, Suppl. B.
(33) Rossnagel, M.S.; Jerome, J.C.; William, D.W. *Handbook of Plasma Processing Technology Fundamentals, Etching, Deposition, and Surface Interactions*; Noyes Publications: Yorktown Heights, NY, 1989.
(34) Capdeville, H. Mesures et modélisation des décharges luminescentes a basse pressions: comportement électrique et pulvérisation des électrodes. Ph.D. Thesis, Orleans University, France, 2001.
(35) Beaudette, T. Caractérisation et Optimisation de lampes planes sans mercure: décharges à barrières diélectriques et luminophores. Ph.D. Thesis, Toulouse University, France, 2009.
(36) Postel, O.B.; Cappelli, M.A. *J. Appl. Phys. Lett.* **2000,** *76,* 544–546.